CLEO CONF 96-24
ICHEP96 PA05-074

Analysis of $B \to J/\psi K$ and $B \to J/\psi K^*$ Decays

CLEO Collaboration

(July 22, 1996)

Abstract

We present the first full angular analysis in the color-suppressed modes $B^0 \to J/\psi K^{*0}$ and $B^+ \to J/\psi K^{*+}$. The data sample of 3.36×10^6 $B\bar{B}$ decays has been collected at the $\Upsilon(4S)$ with the CLEO II detector at the Cornell Electron Storage Ring. This yields the first complete determination of the decay amplitudes of these modes. In addition we update the branching fractions for $B \to J/\psi K$ and $B \to J/\psi K^*$.

D. M. Asner,[1] D. W. Bliss,[1] W. S. Brower,[1] G. Masek,[1] H. P. Paar,[1] J. Gronberg,[2] C. M. Korte,[2] D. J. Lange,[2] R. Kutschke,[2] S. Menary,[2] R. J. Morrison,[2] S. Nakanishi,[2] H. N. Nelson,[2] T. K. Nelson,[2] C. Qiao,[2] J. D. Richman,[2] D. Roberts,[2] A. Ryd,[2] H. Tajima,[2] M. S. Witherell,[2] R. Balest,[3] B. H. Behrens,[3] K. Cho,[3] W. T. Ford,[3] H. Park,[3] P. Rankin,[3] J. Roy,[3] J. G. Smith,[3] J. P. Alexander,[4] C. Bebek,[4] B. E. Berger,[4] K. Berkelman,[4] K. Bloom,[4] D. G. Cassel,[4] H. A. Cho,[4] D. M. Coffman,[4] D. S. Crowcroft,[4] M. Dickson,[4] P. S. Drell,[4] R. Ehrlich,[4] R. Elia,[4] A. D. Foland,[4] P. Gaidarev,[4] B. Gittelman,[4] S. W. Gray,[4] D. L. Hartill,[4] B. K. Heltsley,[4] P. I. Hopman,[4] S. L. Jones,[4] J. Kandaswamy,[4] N. Katayama,[4] P. C. Kim,[4] D. L. Kreinick,[4] T. Lee,[4] Y. Liu,[4] G. S. Ludwig,[4] J. Masui,[4] J. Mevissen,[4] N. B. Mistry,[4] C. R. Ng,[4] E. Nordberg,[4] M. Ogg,[4,*] J. R. Patterson,[4] D. Peterson,[4] D. Riley,[4] A. Soffer,[4] C. Ward,[4] P. Avery,[5] M. Athanas,[5] C. D. Jones,[5] M. Lohner,[5] C. Prescott,[5] S. Yang,[5] J. Yelton,[5] J. Zheng,[5] G. Brandenburg,[6] R. A. Briere,[6] D. Y.-J. Kim,[6] T. Liu,[6] M. Saulnier,[6] R. Wilson,[6] H. Yamamoto,[6] T. E. Browder,[7] F. Li,[7] Y. Li,[7] J. L. Rodriguez,[7] T. Bergfeld,[8] B. I. Eisenstein,[8] J. Ernst,[8] G. E. Gladding,[8] G. D. Gollin,[8] E. Johnson,[8] I. Karliner,[8] M. Palmer,[8] M. Selen,[8] J. J. Thaler,[8] K. W. Edwards,[9] A. Bellerive,[10] D. I. Britton,[10] R. Janicek,[10] D. B. MacFarlane,[10] K. W. McLean,[10] P. M. Patel,[10] A. J. Sadoff,[11] R. Ammar,[12] P. Baringer,[12] A. Bean,[12] D. Besson,[12] D. Coppage,[12] C. Darling,[12] R. Davis,[12] N. Hancock,[12] S. Kotov,[12] I. Kravchenko,[12] N. Kwak,[12] S. Anderson,[13] Y. Kubota,[13] M. Lattery,[13] J. J. O'Neill,[13] S. Patton,[13] R. Poling,[13] T. Riehle,[13] A. Smith,[13] V. Savinov,[13] M. S. Alam,[14] S. B. Athar,[14] Z. Ling,[14] A. H. Mahmood,[14] H. Severini,[14] S. Timm,[14] F. Wappler,[14] A. Anastassov,[15] S. Blinov,[15,†] J. E. Duboscq,[15] R. Fulton,[15] D. Fujino,[15] K. K. Gan,[15] T. Hart,[15] K. Honscheid,[15] H. Kagan,[15] R. Kass,[15] J. Lee,[15] M. Sung,[15] A. Undrus,[15,†] R. Wanke,[15] A. Wolf,[15] M. M. Zoeller,[15] B. Nemati,[16] S. J. Richichi,[16] W. R. Ross,[16] P. Skubic,[16] M. Wood,[16] M. Bishai,[17] J. Fast,[17] E. Gerndt,[17] J. W. Hinson,[17] D. H. Miller,[17] E. I. Shibata,[17] I. P. J. Shipsey,[17] M. Yurko,[17] L. Gibbons,[18] S. D. Johnson,[18] Y. Kwon,[18] S. Roberts,[18] E. H. Thorndike,[18] C. P. Jessop,[19] K. Lingel,[19] H. Marsiske,[19] M. L. Perl,[19] S. F. Schaffner,[19] D. Ugolini,[19] R. Wang,[19] X. Zhou,[19] T. E. Coan,[20] V. Fadeyev,[20] I. Korolkov,[20] Y. Maravin,[20] I. Narsky,[20] V. Shelkov,[20] R. Stroynowski,[20] J. Staeck,[20] I. Volobouev,[20] J. Ye,[20] M. Artuso,[21] A. Efimov,[21] M. Gao,[21] M. Goldberg,[21] R. Greene,[21] F. Frasconi,[21] D. He,[21] S. Kopp,[21] G. C. Moneti,[21] R. Mountain,[21] Y. Mukhin,[21] S. Schuh,[21] T. Skwarnicki,[21] S. Stone,[21] X. Xing,[21] J. Bartelt,[22] S. E. Csorna,[22] V. Jain,[22] S. Marka,[22] A. Freyberger,[23] R. Godang,[23] D. Gibaut,[23] K. Kinoshita,[23] I. C. Lai,[23] P. Pomianowski,[23] S. Schrenk,[23] G. Bonvicini,[24] D. Cinabro,[24] L. Perera,[24] B. Barish,[25] M. Chadha,[25] S. Chan,[25] G. Eigen,[25] J. S. Miller,[25] C. O'Grady,[25] M. Schmidtler,[25] J. Urheim,[25] A. J. Weinstein,[25] and F. Würthwein[25]

[1]University of California, San Diego, La Jolla, California 92093
[2]University of California, Santa Barbara, California 93106
[3]University of Colorado, Boulder, Colorado 80309-0390

[*]Permanent address: University of Texas at Austin.

[†]Permanent address: BINP, RU-630090 Novosibirsk, Russia.

[4]Cornell University, Ithaca, New York 14853
[5]University of Florida, Gainesville, Florida 32611
[6]Harvard University, Cambridge, Massachusetts 02138
[7]University of Hawaii at Manoa, Honolulu, Hawaii 96822
[8]University of Illinois, Champaign-Urbana, Illinois 61801
[9]Carleton University, Ottawa, Ontario, Canada K1S 5B6
and the Institute of Particle Physics, Canada
[10]McGill University, Montréal, Québec, Canada H3A 2T8
and the Institute of Particle Physics, Canada
[11]Ithaca College, Ithaca, New York 14850
[12]University of Kansas, Lawrence, Kansas 66045
[13]University of Minnesota, Minneapolis, Minnesota 55455
[14]State University of New York at Albany, Albany, New York 12222
[15]Ohio State University, Columbus, Ohio 43210
[16]University of Oklahoma, Norman, Oklahoma 73019
[17]Purdue University, West Lafayette, Indiana 47907
[18]University of Rochester, Rochester, New York 14627
[19]Stanford Linear Accelerator Center, Stanford University, Stanford, California 94309
[20]Southern Methodist University, Dallas, Texas 75275
[21]Syracuse University, Syracuse, New York 13244
[22]Vanderbilt University, Nashville, Tennessee 37235
[23]Virginia Polytechnic Institute and State University, Blacksburg, Virginia 24061
[24]Wayne State University, Detroit, Michigan 48202
[25]California Institute of Technology, Pasadena, California 91125

I. INTRODUCTION

The decay $B \to J/\psi K^{(*)}$ proceeds via the color-suppressed internal spectator diagram. Measurement of its rate and polarization therefore provides a test of the factorization hypothesis in decays with internal W-emission. This complements previous tests of factorization in external spectator decays [1].

Phenomenological models based on the factorization hypothesis make predictions about two observables, namely the ratio of vector to pseudoscalar meson production, $R = \mathcal{B}(B \to J/\psi K^*)/\mathcal{B}(B \to J/\psi K)$, and the longitudinal polarization fraction in $B \to J/\psi K^*$, denoted $\Gamma_{\rm L}/\Gamma$. It has been noted [2,3], that form factor models cannot simultaneously explain earlier experimental data on these quantities. The high values of $\Gamma_{\rm L}/\Gamma$ measured by ARGUS [4] and CLEO II [1], with low statistics, are not consistent with factorization and the measured value of R. The CDF collaboration has measured a lower value [5,6] of $\Gamma_{\rm L}/\Gamma$. In this paper we present a more sophisticated analysis using a significantly larger CLEO II data sample.

Since we perform a full fit to the helicity content in $B \to J/\psi K^*$ decays, we can determine the imaginary parts as well as the absolute values of the decay amplitudes. The former are only non-zero in the presence of strong final state interactions (or CP violation), and give additional information about the validity of the factorization hypothesis in internal spectator decays.

Additional interest in $B \to J/\psi K^*$ decays arises because of its role in CP violation measurements at asymmetric B-factories. The decay $B^0 \to J/\psi K^{*0}, K^{*0} \to K^0_S\pi^0$ would be a CP eigenstate if only even or only odd orbital angular momenta are present in the B decays. The CP-even component has a structure similar to that of the CP eigenstate $J/\psi K^0_S$. A purely CP-even decay is thus suited to measure $\sin 2\beta$, where β is one of the angles in the unitarity triangle, the same holds for purely CP-odd decays. Since S, P and D waves may be present, the final state could be an admixture of CP-even and CP-odd eigenstates, which would greatly reduce the sensitivity of the measurement. It is expected that the CP-odd component is small.

In this report we present fits of the angular distributions in the $B^0 \to J/\psi K^{*0}$ and $B^+ \to J/\psi K^{*+}$ modes to extract the full set of decay amplitudes including the P-odd fraction. We also update the branching fractions for these modes as well as those for $B^+ \to J/\psi K^+$ and $B^0 \to J/\psi K^0$. We assume that the production rate of neutral and charge B mesons is the same on the $\Upsilon(4S)$ resonance, in agreement with the actual measured value of $f_+/f_0 = 1.12 \pm 0.20$ [7]. From the branching fractions a value for R is extracted.

II. HELICITY AND TRANSVERSITY FORMALISM

The hadronic decay $B \to J/\psi K^*$ is a transition from a pseudoscalar initial state to a pair of vector mesons. The two vector mesons can exist in three different helicity configurations $(+, 0, -)$, the decay is thus described by 3 complex amplitudes. Imposing a normalization condition and eliminating one overall phase leaves 4 independent parameters, which have to be measured (2 relative amplitudes and 2 phases). The (polar) angular distribution of the decay products in the vector meson rest frame provides a polarization analyzer of the vector meson. Since parity is maximally violated in charged interactions, the amplitudes for + and − helicity states are different.

The full angular distribution of these decays is specified by three angles. In this analysis we use two different sets of angles, one called the helicity basis and the other the transversity basis. For the helicity basis, the three angles are defined to be the polar angle of the l^+ in the J/ψ rest frame, θ_ψ; the polar angle of the K in the K^* rest frame, θ_{K^*}; and the angle between the J/ψ decay plane and the K^* decay plane χ (see Fig. 1). Note, that χ can take on values between 0 and 2π.

The full angular distribution of a B decay in the helicity basis is

$$
\begin{aligned}
\frac{1}{\Gamma}\,\frac{\mathrm{d}^3\Gamma}{\mathrm{d}\cos\theta_\psi\,\mathrm{d}\cos\theta_{K^*}\,\mathrm{d}\chi} = \frac{9}{16\pi}\,\Big\{\, & \frac{1}{4}\,(1+\cos^2\theta_\psi)\sin^2\theta_{K^*}\,\left(\,|H_+|^2+|H_-|^2\,\right) \\
&+ \sin^2\theta_\psi\cos^2\theta_{K^*}\,|H_0|^2 \\
&- \frac{1}{2}\,\sin^2\theta_\psi\sin^2\theta_{K^*}\,[\,\cos 2\chi\,\mathrm{Re}\,(H_+H_-^*) \\
&\qquad\qquad - \sin 2\chi\,\mathrm{Im}\,(H_+H_-^*)\,] \\
&- \frac{1}{4}\,\sin 2\theta_\psi\sin 2\theta_{K^*}\,[\,\cos\chi\,\mathrm{Re}\,(H_+H_0^*+H_-H_0^*) \\
&\qquad\qquad - \sin\chi\,\mathrm{Im}\,(H_+H_0^*-H_-H_0^*)\,]\,\Big\}. \qquad (1)
\end{aligned}
$$

The amplitudes, denoted by H_λ, correspond to the spin configurations of the vector mesons with helicities $\lambda = +, 0, -$.

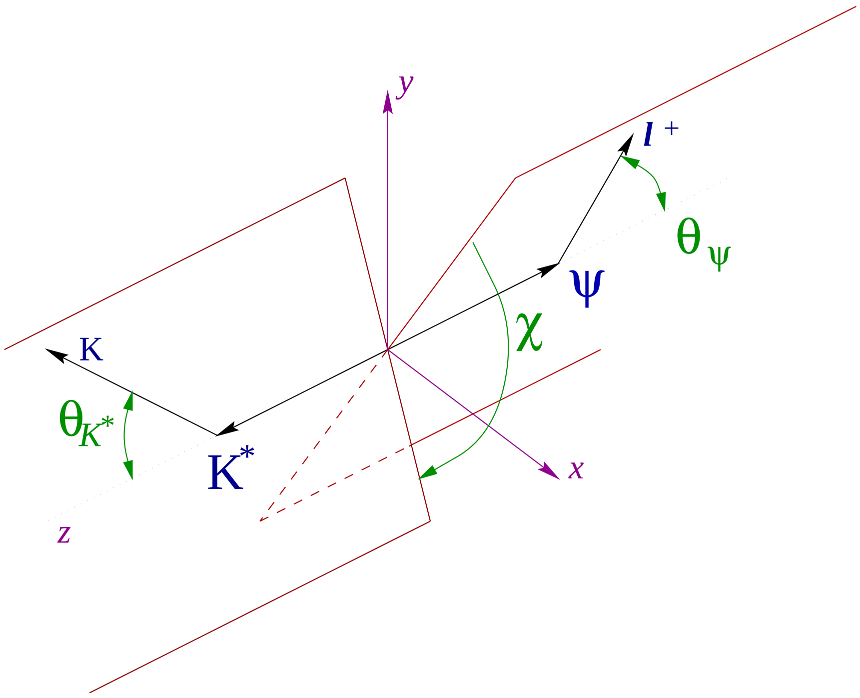

FIG. 1. Definition of helicity angles.

For the $\bar{B}$ decay a similar angular distribution holds for helicity amplitudes H_λ^*. Assuming CP conservation we obtain the following transformations:

$$H_\pm \to H_\mp \quad \text{and} \quad H_0 \to H_0. \tag{2}$$

Inspecting the angular distribution shows that for $\bar{B}$ decays the imaginary parts of the interference terms change sign, which is equivalent to replacing χ by $-\chi$.

The relative longitudinal and transverse polarizations are defined by:

$$\frac{\Gamma_{\rm L}}{\Gamma} = \frac{|H_0|^2}{|H_+|^2 + |H_0|^2 + |H_-|^2}, \tag{3}$$

and

$$\frac{\Gamma_{\rm T}}{\Gamma} = \frac{|H_+|^2 + |H_-|^2}{|H_+|^2 + |H_0|^2 + |H_-|^2}. \tag{4}$$

Thus $\Gamma_{\rm L} + \Gamma_{\rm T} = \Gamma$. The longitudinal polarization can be extracted by integrating Eq. 1 over the χ angle, yielding:

$$\begin{aligned}\frac{1}{\Gamma}\frac{{\rm d}^2\Gamma}{{\rm d}\cos\theta_\psi\,{\rm d}\cos\theta_{K^*}} = &\frac{9}{32}(1+\cos^2\theta_\psi)\sin^2\theta_{K^*}\,(1-\frac{\Gamma_{\rm L}}{\Gamma})\\ &+\frac{9}{8}\sin^2\theta_\psi\cos^2\theta_{K^*}\,\frac{\Gamma_{\rm L}}{\Gamma}.\end{aligned} \tag{5}$$

Performing a one-parameter fit in the $\cos\theta_\psi$-$\cos\theta_{K^*}$ plane determines the longitudinal polarization $\Gamma_{\rm L}/\Gamma$. Using the full angular distribution, on the other hand, allows one to completely determine the helicity amplitudes.

Unless $\Gamma_{\rm L}/\Gamma = 1$, measuring the longitudinal polarization is not sufficient to determine the parity content of $B \to J/\psi K^*$. Following a suggestion of A. Bohr [8], Dighe, Dunietz, Lipkin and Rosner [9] have recently pointed out that a different basis is more convenient for the extraction of parity-even and parity-odd components in a $B \to VV$ decay. The basis is called the transversity basis. A right-handed coordinate system is defined in the J/ψ rest frame. The direction of the K^* in the J/ψ rest frame defines the x-axis. The $K\pi$ plane then fixes the y-axis with $p_y(K) > 0$ and the normal to this plane defines the z-axis (see Fig. 2). The polar angle between l^+ and the z-axis is called the transversity angle $\theta_{\rm tr}$. The projection of the l^+ on the $K\pi$ plane in the J/ψ rest frame and the x-axis define an azimuthal angle $\phi_{\rm tr}$. The third angle, the K^* decay angle θ_{K^*}, is defined in the same way as in the helicity basis. In the transversity basis the three decay amplitudes of the $B \to VV$ decay are then defined by the orientation of the J/ψ polarization vector $\epsilon_{J/\psi}$ in this basis: A_0 for $\epsilon_{J/\psi}$ parallel to $\hat{x}$, $A_\parallel$ for $\epsilon_{J/\psi}$ parallel to $\hat{y}$, and $A_\perp$ for $\epsilon_{J/\psi}$ parallel to $\hat{z}$.

With these definitions the full angular distribution of the $B \to J/\psi K^*$ decay has the following form:

$$\begin{aligned}\frac{1}{\Gamma}\frac{{\rm d}^3\Gamma}{{\rm d}\cos\theta_{\rm tr}\,{\rm d}\cos\theta_{K^*}\,{\rm d}\phi_{\rm tr}} = \frac{9}{32\pi}\,\{&2\cos^2\theta_{K^*}(1-\sin^2\theta_{\rm tr}\cos^2\phi_{\rm tr})\;|A_0|^2\\ &+\sin^2\theta_{K^*}(1-\sin^2\theta_{\rm tr}\sin^2\phi_{\rm tr})\;|A_\parallel|^2\\ &+\sin^2\theta_{K^*}\sin^2\theta_{\rm tr}\sin^2\phi_{\rm tr}\;|A_\perp|^2\\ &-\sin^2\theta_{K^*}\sin 2\theta_{\rm tr}\sin\phi_{\rm tr}\;{\rm Im}\,(A_\parallel^* A_\perp)\end{aligned}$$

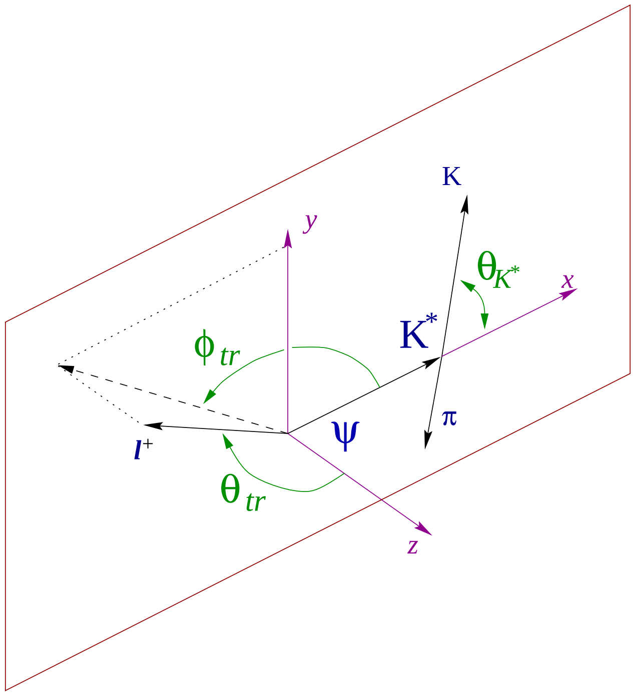

FIG. 2. Definition of transversity angles.

$$
\begin{aligned}
&+\frac{1}{\sqrt{2}} \sin 2\theta_{K^*} \sin^2\theta_{\rm tr} \sin 2\phi_{\rm tr}\ {\rm Re}\,(A_0^* A_\parallel) \\
&+\frac{1}{\sqrt{2}} \sin 2\theta_{K^*} \sin 2\theta_{\rm tr} \cos\phi_{\rm tr}\ {\rm Im}\,(A_0^* A_\perp)\ \}.
\end{aligned} \tag{6}
$$

The decay amplitudes $A_{0,\parallel,\perp}$ are related to the amplitudes H_λ by

$$
H_\pm \;=\; \frac{1}{\sqrt{2}}\,(A_\parallel \pm A_\perp)\,, \qquad H_0 \;=\; -\,A_0\,. \tag{7}
$$

Thus, for the $\bar{B}$ decays $A_\perp$ has to change sign. This can be accomplished by replacing $\phi_{\rm tr}$ by $\phi_{\rm tr} + \pi$. The relations between the angles in the transversity basis and the helicity basis are

$$
\begin{aligned}
\cos\theta_\psi \quad &= \;-\sin\theta_{\rm tr}\ \cos\phi_{\rm tr}, \\
\sin\theta_\psi\ \sin\chi \;&=\; \cos\theta_{\rm tr}, \\
\sin\theta_\psi\ \cos\chi \;&=\; -\sin\theta_{\rm tr}\ \sin\phi_{\rm tr}.
\end{aligned} \tag{8}
$$

The transversity basis has some nice properties. $|A_0|^2 + |A_\parallel|^2$ describe the parity-even (S-wave plus D-wave) and $|A_\perp|^2$ the parity-odd (P-wave) components. Integrating over $\phi_{\rm tr}$ and $\cos\theta_{K^*}$ yields

$$
\frac{1}{\Gamma}\,\frac{{\rm d}\Gamma}{{\rm d}\cos\theta_{\rm tr}} \;=\; \frac{3}{8}\,(1-|A_\perp|^2)\,(1+\cos^2\theta_{\rm tr}) \;+\; \frac{3}{4}\,|A_\perp|^2\ \sin^2\theta_{\rm tr}\,. \tag{9}
$$

The parity-odd component can then be extracted from a one parameter fit.

III. DATA SAMPLE AND EVENT SELECTION

In this analysis we have used a data sample of 3.36×10^6 $B\bar{B}$ events representing an integrated luminosity of 3.14 fb^{-1}. The data were recorded with the CLEO-II detector located at the Cornell Electron Storage Ring. We have also collected a "continuum" data sample, with an integrated luminosity of about 1.6 fb^{-1}, 60 MeV below the $\Upsilon(4S)$ resonance to evaluate non-$b\bar{b}$ backgrounds.

The components of the CLEO-II detector [10] include, starting just outside the beam pipe, three drift chambers, a time-of-flight system, a Tl-doped CsI crystal calorimeter, a 1.5-Tesla superconducting solenoidal magnet, and three layers of muon chambers incorporated in the iron return yoke of the magnet. The charged particle momentum resolution is $(\delta p_t/p_t)^2 = (0.0015p_t)^2 + (0.005)^2$, where p_t is in GeV/c. In the barrel region of the detector, defined as the region where the angle of the shower or track with respect to the beam axis lies between $45°$ and $135°$, the r.m.s. shower energy resolution is $\delta E/E = (0.35/E^{0.75} + 1.9 - 0.1E)\%$, where E is in GeV.

Event selection criteria were optimized for $\Upsilon(4S)$ events with B or $\overline{B}$ decays to charmonium. Events were required to have a reconstructed vertex consistent with the known interaction region, and to have detected visible energy greater than 15% of the center-of-mass energy. To suppress background from QED processes we required at least five reconstructed charged tracks.

IV. J/ψ RECONSTRUCTION

We reconstruct J/ψ mesons via their decays $J/\psi \to e^+e^-$ and $J/\psi \to \mu^+\mu^-$. Leptons are required to have a momentum greater than 0.8 GeV, which is the lower kinematically allowed limit for $B \to J/\psi X$ decays.

Electrons are identified by combining information from several detector components. The energy deposited in the calorimeter must be consistent with the corresponding track momentum, and the specific ionization (dE/dx) as measured by the main drift chamber must be consistent with that expected for an electron.

Muons are identified by matching reconstructed charged tracks to hits in the muon chambers. At least one of the muons is required to penetrate five nuclear interaction lengths of iron while the other is required to have penetrated at least three interaction lengths.

The data show signals in both modes (Fig. 3). The tail to lower invariant masses is due to final state radiation and bremsstrahlung; this effect is much more pronounced for $J/\psi \to e^+e^-$ than for $J/\psi \to \mu^+\mu^-$.

We require the dimuon invariant mass to be within 45 MeV around the J/ψ mass. This corresponds to a 3σ selection. For the dielectron invariant mass we require $-150\,\mathrm{MeV} < m_{ee} - m_{J/\psi} < 45\,\mathrm{MeV}$ to allow for the radiative tail. The J/ψ energy resolution is improved by a factor of $5-6$ after performing a kinematic fit of the dilepton mass to the nominal J/ψ mass. The kinematic fit does not affect the measurements of the angles. The resolution of the angle measurements is better than 0.02 for all decay angles.

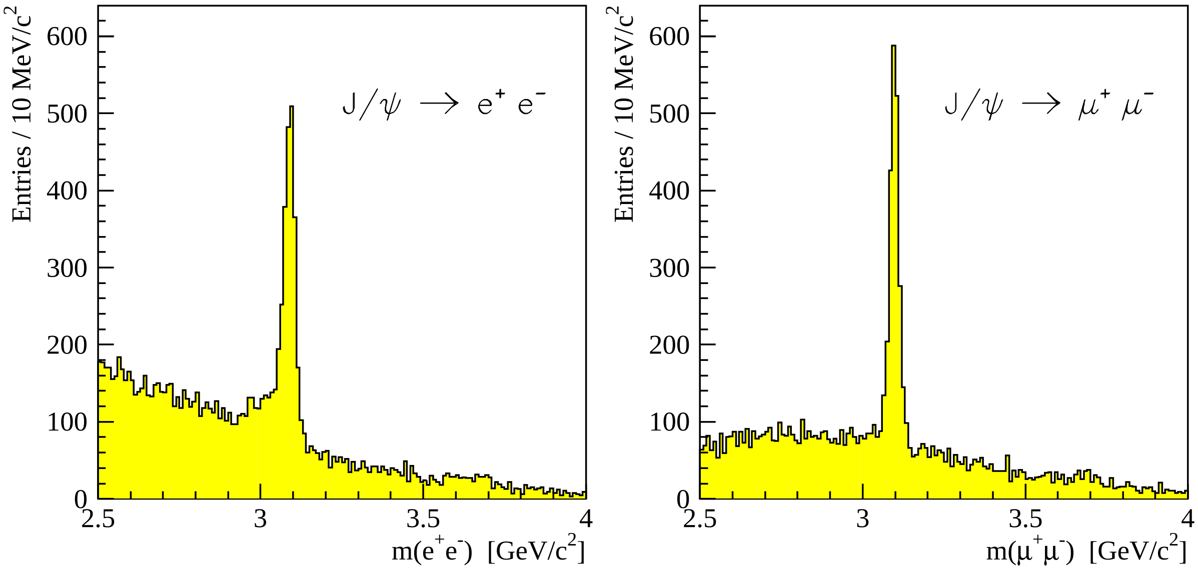

FIG. 3. Inclusive signals of $J/\psi \to e^+e^-$ and $J/\psi \to \mu^+\mu^-$

V. K AND K^* RECONSTRUCTION

We require that charged hadron candidates have dE/dx measurements that lie within three standard deviations of the expected values. We reconstruct K^0_S candidates through the decay to $\pi^+\pi^-$ and we reconstruct π^0 candidates through the decay to $\gamma\gamma$.

Candidate K^* mesons are formed in the modes $K^{*+} \to K^+\pi^0$, $K^{*+} \to K^0_S\pi^+$, $K^{*0} \to K^+\pi^-$ and $K^{*0} \to K^0_S\pi^0$. The K^* candidates are required to have an invariant mass within 75 MeV of the nominal K^* mass.

VI. B CANDIDATES

At the Υ(4S) resonance, the energy of a B meson must equal the beam energy. We require that the energy difference between the B candidate and the beam energy ($|\Delta E|$) be less than 45 MeV for $J/\psi K^+$ and $J/\psi K^0_S$, less than 30 MeV for $J/\psi(K^+\pi^-)^*$ and $J/\psi(K^0_S\pi^+)^*$, and less than 60 MeV for $J/\psi(K^+\pi^0)^*$ and $J/\psi(K^0_S\pi^0)^*$. These ranges correspond to approximately 3σ in ΔE.

For each $B \to J/\psi K^*$ candidate a probability is constructed. For modes with a π^0, $|\Delta E|$ and the measured π^0 mass are used. For modes with a charged pion, $|\Delta E|$, dE/dx and time-of-flight information are used for both the pion and kaon, if available. This probability is used to select candidates in cases where an event has more than one candidate per mode. We keep only the candidate with the highest probability. This selection has been designed to suppress signal events with misidentified particles, which may happen, for example, by including a random π^0 or swapping of K^+ and π^-. In these cases incorrect angular information is inferred. To further suppress backgrounds from feed-across and mistags, we require the probability to be greater than 1%.

To suppress feed-across background in the $B \to J/\psi K^*$, with $K^* \to K\pi^0$ modes due to random or fake slow π^0's, we require that the K^* decay angle satisfies $\cos\theta_{K^*} < 0.7$ in these decays. This is equivalent to a constraint on the π^0 momentum, corresponding to a minimum p_{π^0} of about 200 MeV. We choose a constraint on the decay angle rather than on the momentum because we are looking at the efficiency as a function of the K^* decay angle.

The resolution on the beam energy is much better than the resolution on the B candidate energy. Thus we substitute the beam energy in the calculation of the B-candidate mass (referred to as the "beam-constrained mass"). The beam-constrained mass distributions with all selection criteria applied are shown in Fig. 4. For $m_B > 5.27$ we obtain the yields listed in Table I.

Decay mode		Yield	Efficiency [%]
$B^+ \to J/\psi K^+$	$J/\psi \to e^+e^-$	73	34.9 ± 1.0
	$J/\psi \to \mu^+\mu^-$	80	34.1 ± 1.0
$B^0 \to J/\psi K^0_S$	$J/\psi \to e^+e^-$	25	27.9 ± 1.1
	$J/\psi \to \mu^+\mu^-$	9	25.7 ± 1.1
$B^+ \to J/\psi(K^+\pi^0)^{*+}$	$J/\psi \to e^+e^-$	16	12.9 ± 0.1
	$J/\psi \to \mu^+\mu^-$	20	11.5 ± 0.1
$B^+ \to J/\psi(K^0_S\pi^+)^{*+}$	$J/\psi \to e^+e^-$	9	17.0 ± 0.2
	$J/\psi \to \mu^+\mu^-$	9	15.7 ± 0.2
$B^0 \to J/\psi(K^+\pi^-)^{*0}$	$J/\psi \to e^+e^-$	45	23.2 ± 0.2
	$J/\psi \to \mu^+\mu^-$	40	21.0 ± 0.2
$B^0 \to J/\psi(K^0_S\pi^0)^{*0}$	$J/\psi \to e^+e^-$	2	9.3 ± 0.1
	$J/\psi \to \mu^+\mu^-$	5	8.0 ± 0.1

TABLE I. Total yields for $m_B > 5.27$ GeV and detection efficiencies for the various decay modes. The efficiencies for $B \to J/\psi K^*$ assume flat angular distributions.

The efficiencies are also given in Table I. For the $B \to J/\psi K^*$ modes the efficiency is dependent on the longitudinal polarization. The efficiencies in Table I are for decays with flat angular distributions.

VII. BACKGROUNDS

A. $B \to J/\psi K^*$ Feed-Across

Feed-across from one $B \to J/\psi K^*$ mode to another is the most severe background in the $B \to J/\psi K^*$ modes, since for feed-across events both the total energy and the beam-constrained mass are very close to the signal region. Mistagged $B \to J/\psi K^*$ events in which the correct mode has been identified, but which contain an incorrect pion, an incorrect gamma, or have the kaon and the pion swapped (in case of $B \to J/\psi(K^+\pi^-)^*$) are treated as feed-across background, because the decay angle information may be incorrect.

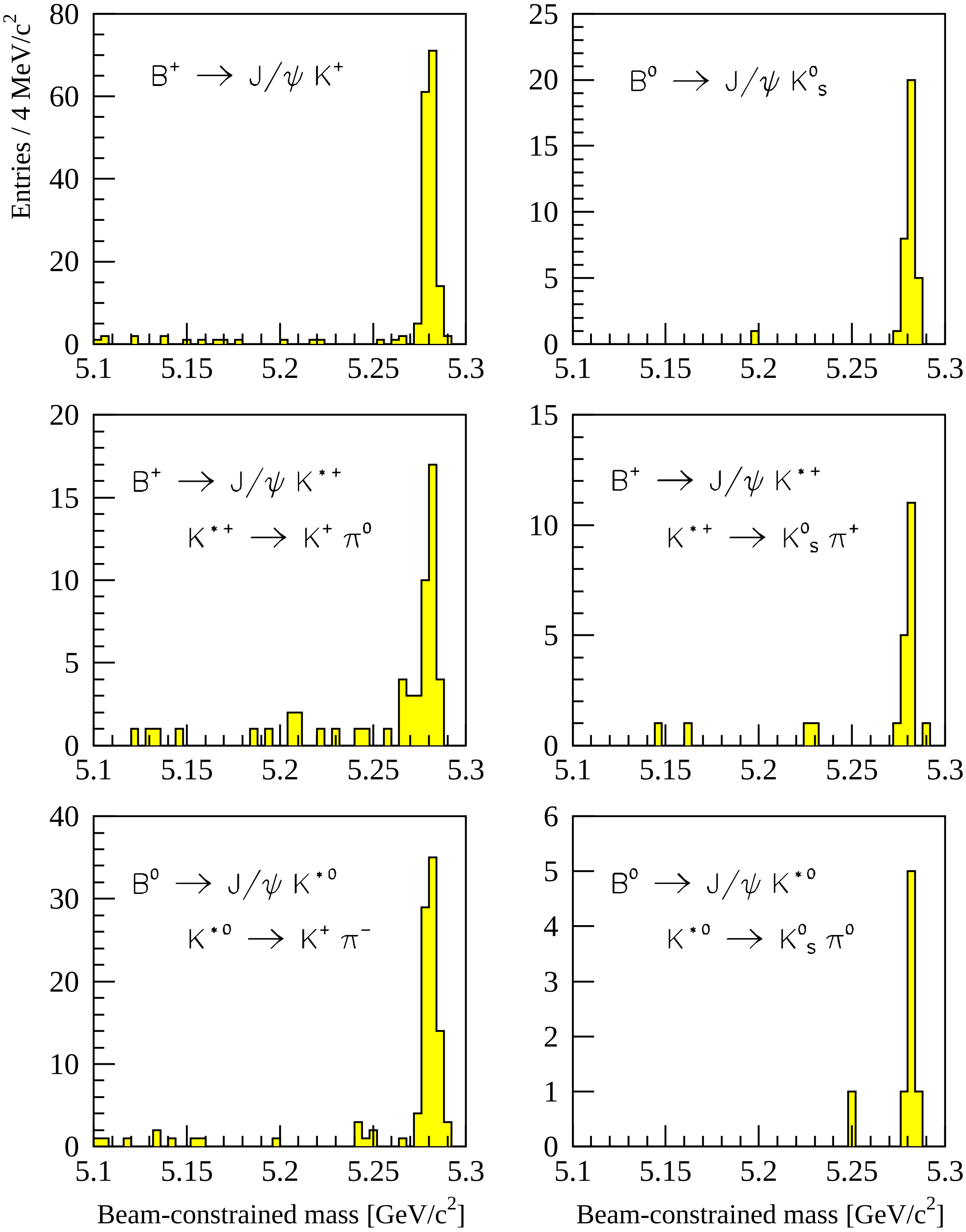

FIG. 4. Beam-constrained mass distributions for all modes, summed over both J/ψ decay modes.

The biggest source of feed-across background is from swapping a real or fake slow pion for the correct one. Thus most of the background is where the K^* decay angle is near $-\pi$. As mentioned before, this background is reduced by imposing an upper bound on the K^* decay angle for events with π^0's. The fraction of feed-across events in the signal region is 8.0%.

B. Background in the K^* Mass Region

There might be a contribution from non-resonant $B \to J/\psi K\pi$ decays in the K^* signal region, though neither the previous CLEO measurement [1] nor CDF [5] found events in the K^* mass sidebands. However, if we examine the $K\pi$ invariant mass (Fig. 5), we find an excess of events between 1.1 and 1.45 GeV. This excess does not have the shape one would expect from a normal non-resonant phase space distribution, which would extend up to about 2.2 GeV. We have considered the following possible origins for the events with $m_{K\pi}$ above 1.1 GeV (see Fig. 6):

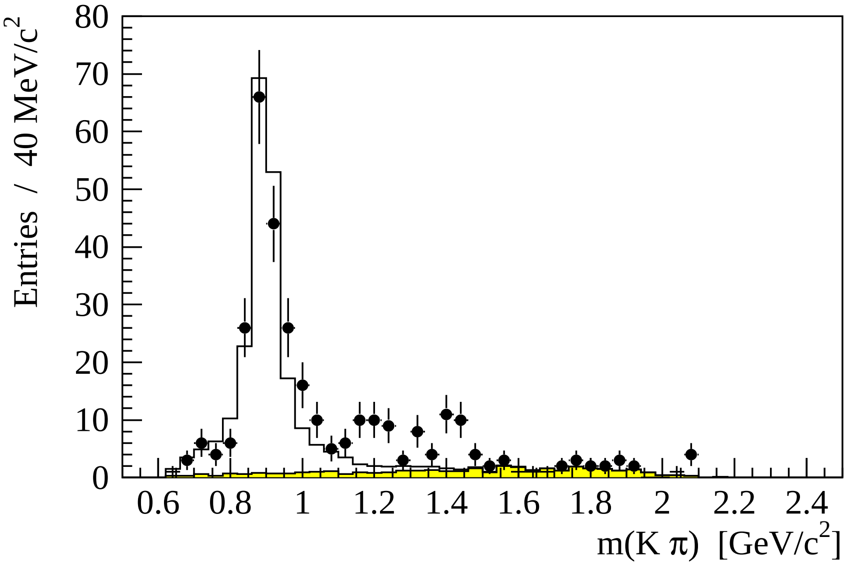

FIG. 5. The $K\pi$ mass distribution for $m_B > 5.27$ GeV. Shown are the data points, the fitted K^* mass peak incl. feed-across (empty histogram) and the combinatorial background (shaded histogram).

- Feed-down from higher modes like $B \to J/\psi K^*\pi$ or $B \to J/\psi K\rho$ is ruled out by the B energy distribution (see Fig. 6 (a)). In cases when at least a pion is missed the B energy will be too small to enter the signal region. Events could leak into our energy window, but they would mostly populate the low energy region. Our events, on the other hand, are distributed symmetrically around the beam energy; thus, this explanation is rather unlikely.
- The same argument holds for feed-through from $B \to J/\psi K$: We would expect a very asymmetric distribution in the B candidate energy. In addition, no significant

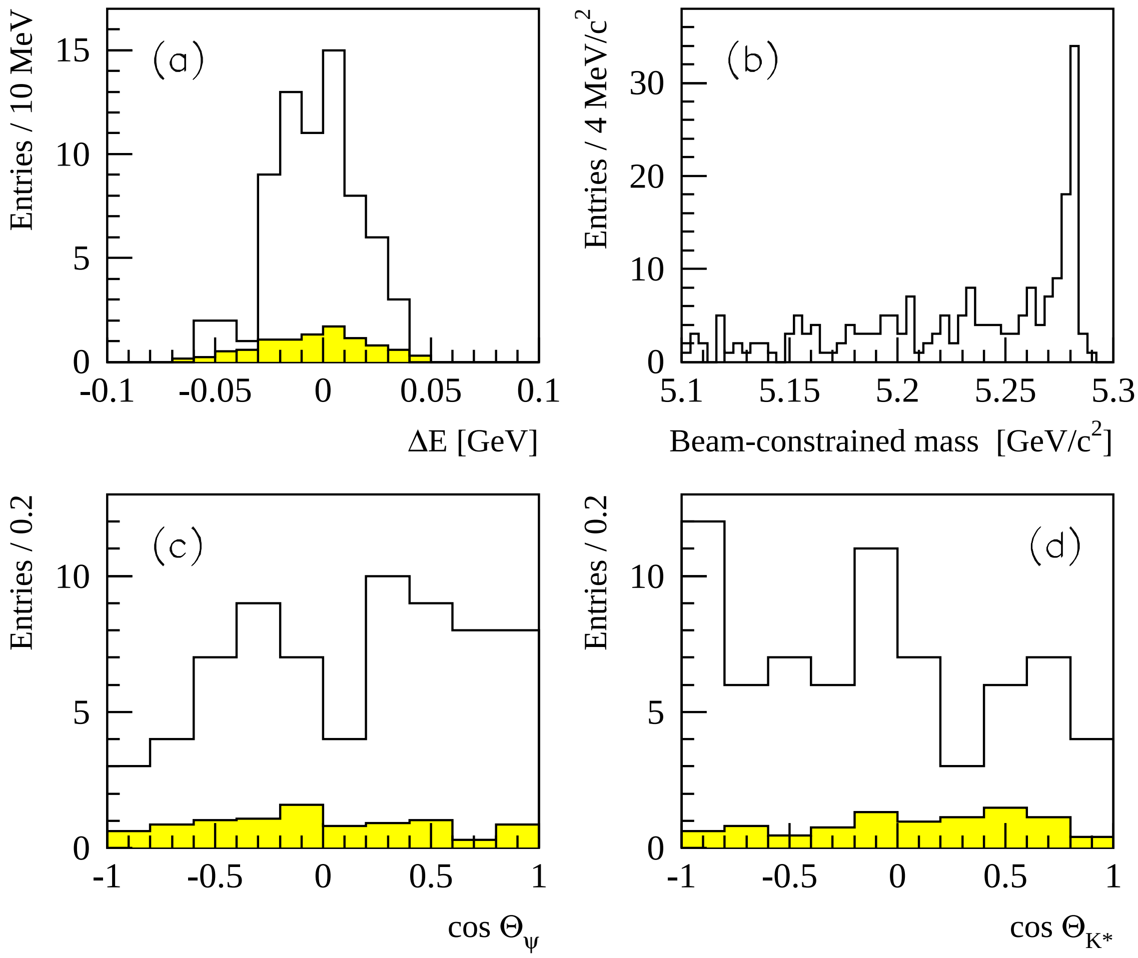

FIG. 6. Distributions of (a) ΔE, (b) beam-constrained mass, (c) $\cos\theta_\psi$ and (d) $\cos\theta_{K^*}$ for events in the K^* mass sideband between 1.1 GeV and 1.45 GeV (white), and for scaled events from the B mass sideband (shaded).

feed-through is found in the Monte Carlo simulation.

- Decays via higher resonances like $B \to J/\psi K^*(1410)$, $B \to J/\psi K_0^*(1430)$ or $B \to J/\psi K_2^*(1430)$ with $K^* \to K\pi$ could produce a more symmetric $K\pi$ mass distribution around 1.42 GeV. There are no resonances in the critical region which decay to $K\pi$. In addition, for $B \to J/\psi K_0^*(1430)$ we would expect fully polarized decays. We do not see a significant polarization for the problematic events (Fig. 6 (c) and (d)). However, we cannot completely rule out the possibility of an interference between the different K^* resonances as the origin of the observed excess.

- Feed-across from $B \to J/\psi K^*$ does have a tail that extends to higher $m_{K\pi}$. However, this tail dies out quickly. The fitted K^* mass peak in Fig. 5 does include the K^* feed-across, which cannot explain the excess events.

We also checked the $K\pi$ invariant mass distribution using generic $B\bar{B}$ Monte Carlo events, which contain a variety of non-resonant $B \to J/\psi X$ decays. We see the $B \to J/\psi(K\pi)_{\mathrm{NR}}$ events are evenly distributed over the whole $m_{K\pi}$ phase space region, but we do not see any excess between 1.1 and 1.5 GeV.

Since we cannot attribute the high mass excess in the $K\pi$ mass distribution to any of the sources listed above, we will treat those events as non-resonant $B \to J/\psi K\pi$ decays. We model them with a straight line for $m_{K\pi} < 1.45$ GeV crossing zero at $m_{K\pi} = m_K + m_\pi = 0.63$ GeV. Performing the fit to the combined set of the 4 $J/\psi K^*$ modes, and letting the normalization of both the resonant and non-resonant decays float, we obtain a non-resonant contribution of 6.4% in the K^* mass region. Since this is only a very crude estimate of the amount and the shape of the non-resonant background, we assign an systematic error of $\pm 100\%$ to this value.

C. Background from Other $B \to J/\psi X$ Decays

Other misidentified $B \to J/\psi X$ decays like $B \to J/\psi K^*\pi$ do not contribute much to the background, since they usually lie outside the energy window. CLEO has seen 9 events in the signal region for $B \to J/\psi\rho^0$ [11]. If a pion from the ρ is misidentified as a kaon, the "$K^+\pi^-$" mass could fall in the K^* region but these events would fail the $|\Delta E|$ energy criterion. Feed-across between the $J/\psi K$ and $J/\psi K^*$ modes is also suppressed by the requirement on $|\Delta E|$. Furthermore the contributions are flat in the beam-constrained mass (see left column of Fig. 7). We, therefore, just include them in the combinatorial background (see next paragraph).

D. Combinatorial Background

We define combinatorial backgrounds to be events, which do not contain a $J/\psi \to l^+l^-$ decay. In the Monte Carlo simulation we see very few such events (see right column of Fig. 7), their beam-constrained mass distribution can easily be modeled with a constant plus a parabola at the phase space limit. Most of the combinatorial background comes from $B\bar{B}$ decays, not from continuum events.

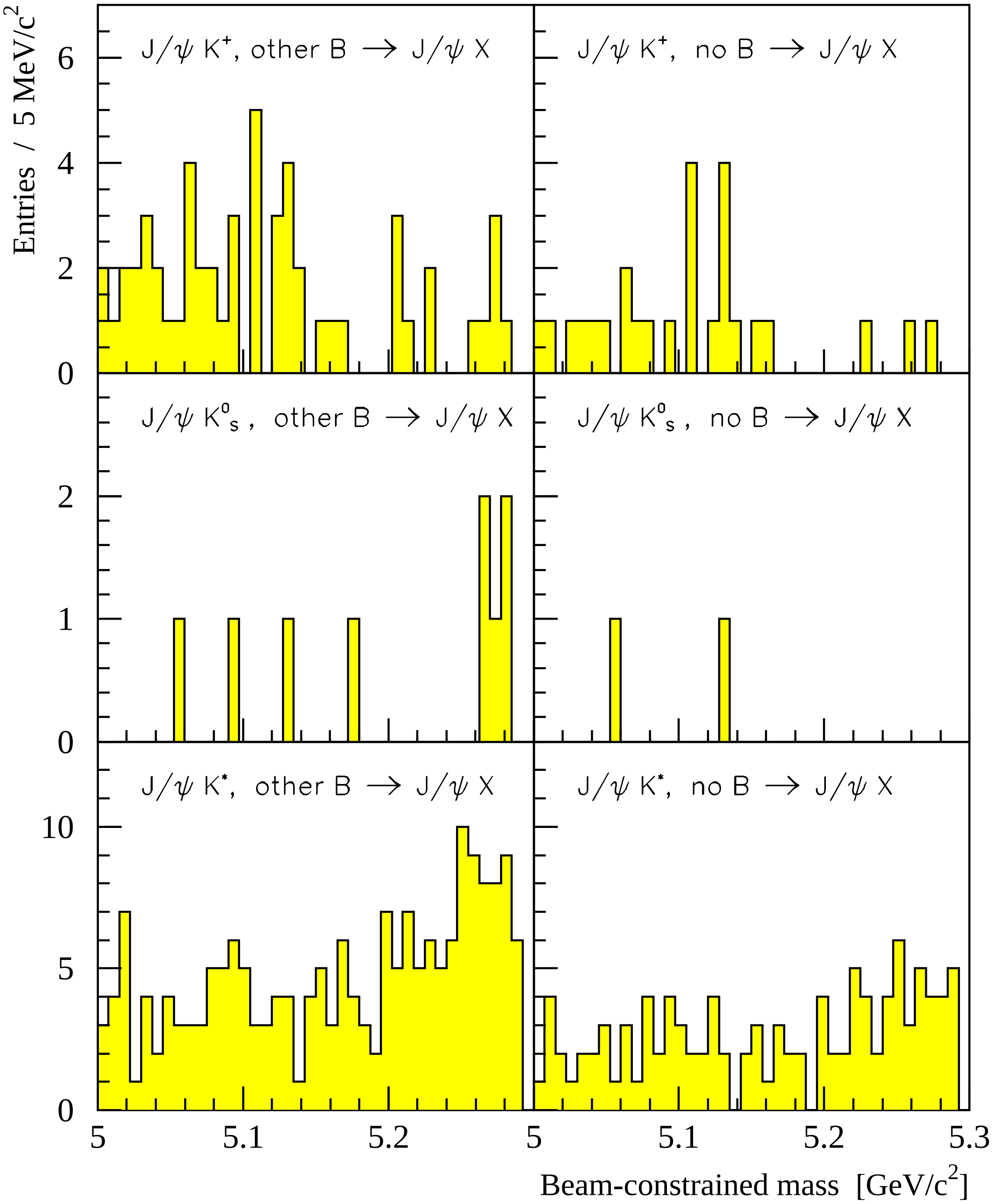

FIG. 7. Backgrounds from $B \to J/\psi X$ decay modes other than the mode looked for (left) and $B \to$ non$-J/\psi$ decays (right). To generate these distributions we used a generic $B\bar{B}$ Monte Carlo sample of approximately 3.2 times the data sample size.

VIII. FIT PROCEDURES FOR $B \to J/\psi K^*$ DECAY AMPLITUDES

We perform a full four-parameter fit in the transversity basis to the angular distributions. As consistency checks, we perform two one-parameter fits, one in the helicity basis (measuring Γ_L/Γ) and one in the transversity basis (measuring the P-wave fraction).

We must correct our data for detection efficiency. To obtain the efficiency ϵ as a function of all three angles, a large Monte Carlo sample (120,000 events/K^* mode) is divided into a $20 \times 20 \times 10$ grid in $\cos\theta_{\rm tr}$, $\cos\theta_{K^*}$ and $\phi_{\rm tr}$. The efficiency is fitted with polynomials in three dimensions including all correlations. For each $J/\psi K^*$ final state the efficiency is fitted separately. The efficiency distributions are nearly flat in all angles except the K^* decay angle, in which the efficiency drops at high $\cos\theta_{K^*}$ because of the decrease in the slow pion efficiency.

To fit the decay amplitudes in the transversity basis, an unbinned maximum likelihood fit is performed according to

$$
\begin{aligned}
N_{\rm data}(m_B, x, y, z) \;=\; & N_{b\bar{b}}\, \mathcal{B}(B \to J/\psi K^*)\, \mathcal{B}(J/\psi \to l^+l^-)\, \mathcal{B}(K^*\text{decay}) \\
& \times G(m_B) \cdot \frac{1}{N}\, \epsilon\,(x,y,z)\, \frac{\mathrm{d}\Gamma}{\mathrm{d}x\mathrm{d}y\mathrm{d}z}(x,y,z) \\
& + N_{b\bar{b}}\, \mathcal{B}(B \to J/\psi K^*)\, \mathcal{B}(J/\psi \to l^+l^-) \\
& \times \sum_{K^*\text{modes}} \mathcal{B}(K^*\text{decay}) f^i_{\rm feed-across}(m_B)\, \epsilon^i_{\rm feed-across}(x,y,z) \\
& + N_{\rm non-res}\, f_{\rm non-res}(m_B, x, y, z) \\
& + N_{\rm comb-bkg}\, f_{\rm comb-bkg}(m_B)\,.
\end{aligned}
\tag{10}
$$

The three transversity angles $\cos\theta_{\rm tr}$, $\cos\theta_{K^*}$, and $\phi_{\rm tr}$ are denoted as x, y, and z. Both $\mathcal{B}(K^* \to K\pi)$ and $\mathcal{B}(J/\psi \to l^+l^-)$ are the measured branching ratios for the corresponding decays [12]. $G(m_B)$ is a normalized Gaussian describing the beam-constrained mass distribution with a variable mean and the width obtained from Monte Carlo simulation. The efficiencies $\epsilon^i_{\rm feed-across}(x,y,z)$ and the line shape $f^i_{\rm feed-across}(m_B)$ for feed-across are parameterized by fitting Monte Carlo distributions. The normalization $N_{\rm non-res}$, the line shape and the angular distribution $f_{\rm non-res}(m_B, x, y, z)$ for non-resonant events are obtained from fits to the K^* mass sideband. Finally, the normalization $N_{\rm comb-bkg}$ of the combinatorial background is allowed to float in the fit, and the line shape $f_{\rm comb-bkg}(m_B)$ has been described in Sec. VII D. All functions f in Eq. 10 are normalized to 1. The overall normalization N, is defined by

$$
N \;=\; \int \mathrm{d}x\mathrm{d}y\mathrm{d}z\, \epsilon\,(x,y,z)\, \frac{\mathrm{d}\Gamma}{\mathrm{d}x\mathrm{d}y\mathrm{d}z}\,(x,y,z)\,. \tag{11}
$$

The free parameters in the fits are the parameters of the angular distributions, the branching fraction $\mathcal{B}(B \to J/\psi K^*)$, the mean of the m_B distribution and the normalization $N_{\rm comb-bkg}$ of the combinatorial background. In simultaneous fits with more than one fitted mode, each mode has its own combinatorial background normalization. Including the beam-constrained mass distribution in the fit ensures the correct treatment of the background events and automatically adjusts the branching ratio measurement for the polarization dependence of the efficiency.

IX. RESULTS

A. $\mathcal{B}(B^+ \to J/\psi K^+)$ and $\mathcal{B}(B^0 \to J/\psi K^0)$

The decay modes $B^+ \to J/\psi K^+$ and $B^0 \to J/\psi K^0_S$ have very low background levels. clean. For the latter we find only 3 background events with $m_B > 5$ GeV. The results from the fit are given in Table II with the fits shown in Fig. 8. As a consistency check we performed fits to these modes with the fraction of longitudinal polarization floating, giving Γ_L/Γ compatible with 1 in both modes, as expected since the kaon has spin zero.

B Decay Mode	Branching Fraction $[\times 10^3]$
$B^+ \to J/\psi K^+$	1.08 ± 0.09
$B^0 \to J/\psi K^0$	$0.92\ ^{+0.17}_{-0.15}$

TABLE II. Branching ratios for $B \to J/\psi K^+$ and $B \to J/\psi K^0$.

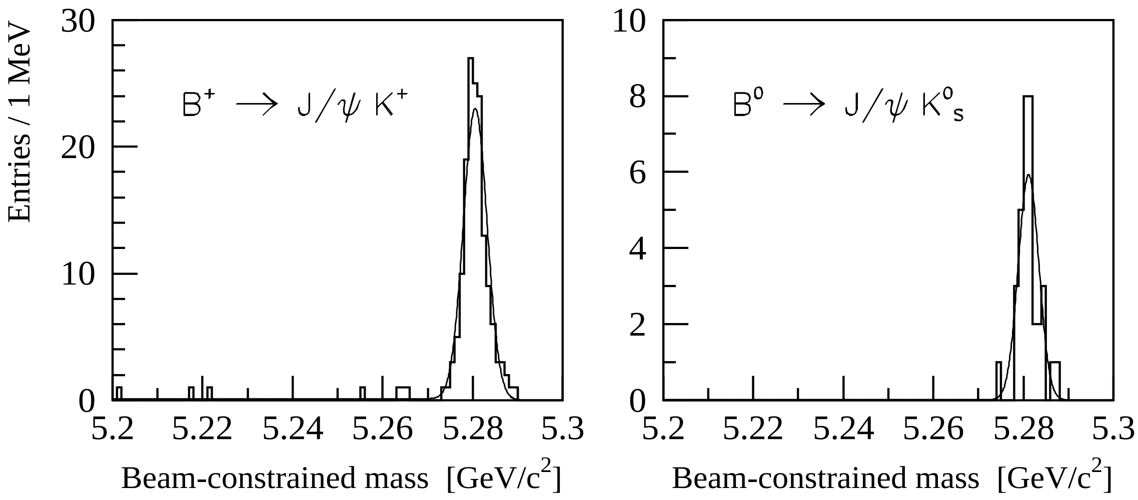

FIG. 8. Fits of $B^+ \to J/\psi K^+$ and $B^0 \to J/\psi K^0$ mass distributions.

B. $\mathcal{B}(B^+ \to J/\psi K^{*+})$, $\mathcal{B}(B^0 \to J/\psi K^{*0})$ and Decay Amplitudes

Table III gives the results of the full 3-dimensional, 4-parameter fit in the transversity basis. We choose to fit for $|A_0|^2 = \Gamma_L / \Gamma$, $|A_\perp|^2 = |P|^2$ and the phases of $A_\perp$ and $A_\parallel$ where we have defined A_0 to be real. Figure 9 shows the results of the fit. The full fit in the transversity basis converges very well. As shown in Table IV, the correlations between the fit parameters are small. We define $\phi(A_0) \equiv 0$, and observe that all three decay amplitudes have imaginary parts compatible with 0, consistent with the absence of strong final-state interactions.

Taking the values found in the fit to the transversity variables we can calculate the coefficients in the helicity basis. We find $|H_+|^2$ to be 0.01 and $|H_-|^2$ to be 0.47 with both H_+ and H_- having small imaginary components. In a fit with the helicity basis, the fact that H_+ is consistent with zero means that the phase of H_+ is not well defined. In addition, if H_+ and H_- have no imaginary parts, then it is not possible to distinguish between the two by a fit in the helicity basis (see Eq. 1). For these reasons we choose to do a full fit only for the $A_{0,\perp,\parallel}$ amplitudes.

For a consistency check we repeated the full fit to the decay amplitudes using helicity angles rather than transversity angles. As expected, both sets of results are in agreement.

For the 1-dimensional helicity fit the results are given in Table V, and shown in Fig. 10. The result of the 1-dimensional fit in the transversity basis is given in Table VI and shown in Fig. 11. The values found in the 1-dimensional fits are in good agreement with the those found in the full 3-dimensional fit.

An independent angular analysis with the same data sample has been performed, which used a completely different fit technique. The results obtained for the helicity parameters are consistent with those reported here.

B Decay Mode	Parameter	Value
$B^+ \to J/\psi K^{*+}$	$10^3 \times \mathcal{B}(B \to J/\psi K^{*+})$	1.41 ± 0.20
	$\|A_0\|^2 = \Gamma_L / \Gamma$	0.53 ± 0.11
	$\|A_\perp\|^2 = \|P\|^2$	$0.11 ^{+0.15}_{-0.06}$
	$\phi(A_\perp)$	1.57 ± 2.44
	$\phi(A_\parallel)$	3.14 ± 0.67
$B^+ \to J/\psi K^{*0}$	$10^3 \times \mathcal{B}(B \to J/\psi K^{*0})$	1.32 ± 0.14
	$\|A_0\|^2 = \Gamma_L / \Gamma$	0.52 ± 0.08
	$\|A_\perp\|^2 = \|P\|^2$	0.18 ± 0.09
	$\phi(A_\perp)$	$-0.53 ^{+0.53}_{-0.61}$
	$\phi(A_\parallel)$	3.00 ± 0.46
$B^+ \to J/\psi K^*$ combined	$10^3 \times \mathcal{B}(B \to J/\psi K^*)$	1.35 ± 0.12
	$\|A_0\|^2 = \Gamma_L / \Gamma$	0.52 ± 0.07
	$\|A_\perp\|^2 = \|P\|^2$	0.16 ± 0.08
	$\phi(A_\perp)$	-0.11 ± 0.46
	$\phi(A_\parallel)$	3.00 ± 0.37

TABLE III. Resulting decay amplitudes from the full fit to the transversity angles. The correlation coefficients of the combined fit are given in Table IV.

	$\|A_0\|^2$	$\|A_\perp\|^2$	$\phi(A_\perp)$	$\phi(A_\parallel)$
$\mathcal{B}(B \to J/\psi K^*)$	0.15	-0.04	-0.01	-0.01
$\|A_0\|^2 = \Gamma_L / \Gamma$		-0.33	-0.07	0.00
$\|A_\perp\|^2 = \|P\|^2$			-0.14	-0.04
$\phi(A_\perp)$				0.59

TABLE IV. Correlation coefficients of the full fit to the transversity angles.

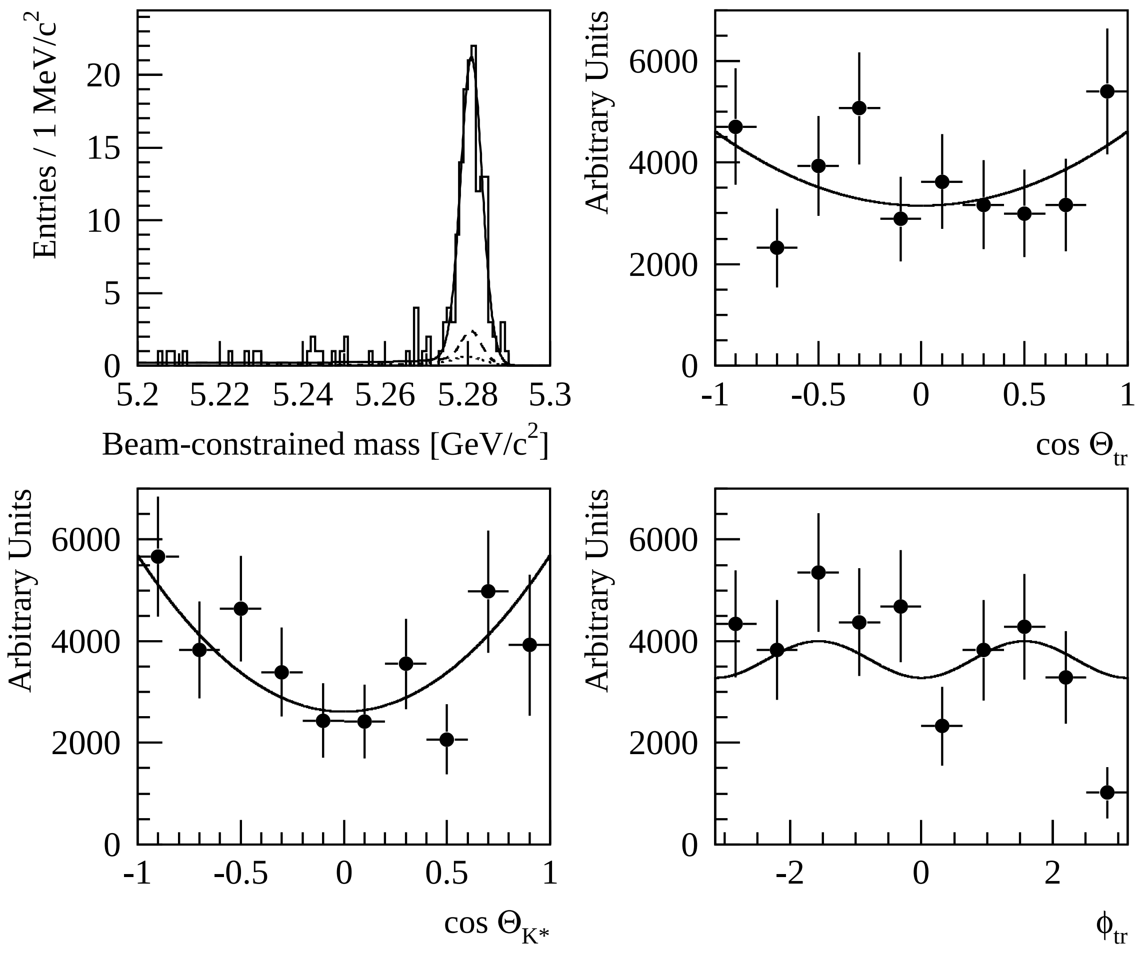

FIG. 9. Full fit using the information from all three transversity angles. In the plot of the beam-constrained mass the fit is the solid line, the sum of all backgrounds is dashed and the $B \to J/\psi K^*$ feed-across is dotted. The angular distributions are background subtracted and efficiency corrected.

B Decay Mode		Γ_L / Γ
$B^+ \to J/\psi K^{*+}$	$K^{*+} \to K^+ \pi^0$	0.44 ± 0.16
$B^+ \to J/\psi K^{*+}$	$K^{*+} \to K^0_S \pi^+$	$0.58\ ^{+0.16}_{-0.17}$
$B^0 \to J/\psi K^{*0}$	$K^{*0} \to K^+ \pi^-$	0.48 ± 0.09
$B^0 \to J/\psi K^{*0}$	$K^{*0} \to K^0 \pi^0$	0.84 ± 0.22
all K^* modes		0.51 ± 0.07

TABLE V. Results for Γ_L/Γ from the fit to the helicity angles $\cos\theta_\psi$ and $\cos\theta_{K^*}$.

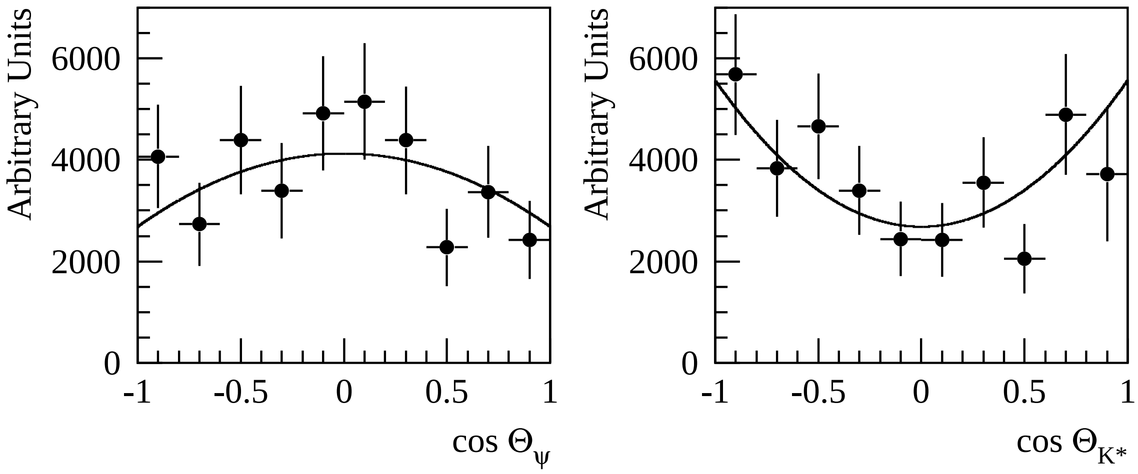

FIG. 10. Fit of Γ_L/Γ using the helicity angles $\cos\theta_\psi$ and $\cos\theta_{K^*}$. The data are background subtracted and efficiency corrected.

Decay Mode		$\lvert A_\perp \rvert^2$
$B^+ \to J/\psi K^{*+}$	$K^{*+} \to K^+ \pi^0$	0.45 ± 0.31
$B^+ \to J/\psi K^{*+}$	$K^{*+} \to K^0_S \pi^+$	0.31 ± 0.43
$B^0 \to J/\psi K^{*0}$	$K^{*0} \to K^+ \pi^-$	0.03 ± 0.18
all K^* modes		0.21 ± 0.14

TABLE VI. Results for the P-odd fraction $|A_\perp|^2$ from the fit to the transversity angle $\cos\theta_{tr}$.

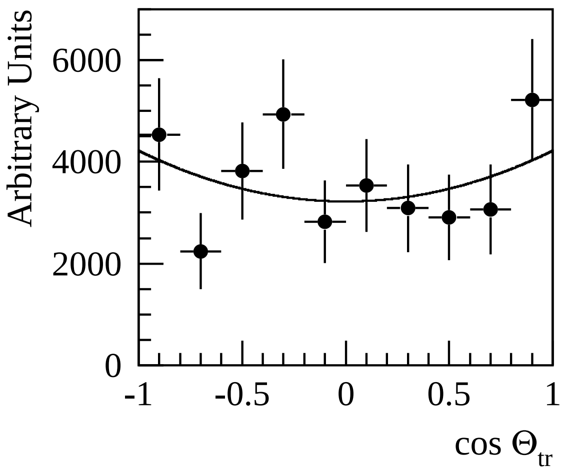

FIG. 11. Fit of the P-odd fraction $|A_\perp|^2$ using the transversity angle $\cos\theta_{\rm tr}$. The data are background subtracted and efficiency corrected.

X. SYSTEMATIC UNCERTAINTIES

In the following section we describe the sources of significant systematic uncertainties. The values of the systematic errors on the branching ratio measurements are tabulated in Table VII.

- Tracking efficiency:
  We assign a 1% error per track on the track fitting and finding efficiency. These errors are added linearly, resulting in total errors of $2\% - 4\%$ depending on the mode. In addition we assign 5% errors on the π^0 and the K^0_S finding efficiency, which are added in quadrature to the error on the charged tracks.

- Lepton identification efficiency:
  We assign a 2.7% error per lepton track (added linearly) on the branching ratio measurements to account for the uncertainty in the lepton identification.

- Efficiency parameterization:
  Our knowledge of the shape of the $B \to J/\psi K^*$ efficiency parameterization is limited by Monte Carlo statistics as well as by our choice of the fitting function. We estimate a systematic error on the parameterization in $\cos\theta_{\rm tr}$, $\phi_{\rm tr}$ and of the correlation terms by comparing with the results of fits obtained by using flat distributions. To estimate the systematic error due to the uncertainty in the efficiency in $\cos\theta_{K^*}$ we fit using only events with $\cos\theta_{K^*} < 0.7$ for the $K^* \to K\pi^\pm$ modes, i.e. excluding the region with the efficiency drop. For the $K^* \to K\pi^0$ modes, where this K^* angle cut is already imposed, we take the systematic error from the $K^* \to K\pi^\pm$ modes.

- Normalization and shape of $B \to J/\psi K^*$ feed-across:
  The normalization of the $B \to J/\psi K^*$ feed-across background is determined from the fitted $B \to J/\psi K^*$ branching fractions. The only additional uncertainty is the modeling of mistags in the Monte Carlo simulation. We conservatively assign an error

of $\pm 50\%$ on the mistag probability, which includes the uncertainty in the shape of $B \to J/\psi K^*$ feed-across.

- Polarization of $B \to J/\psi K^*$ feed across:
  The feed-across background in the $J/\psi K^*$ channels may be carrying polarization information. In particular, the J/ψ decay angle is not changed much when a K^* is misconstructed. The amount of polarization in the background differs for different angles. This makes the polarization of the feed-across very difficult to model. Instead we assume a flat polarization distribution of the feed-across events for the main analysis. On the other hand, assuming that the feed-across events carry the same polarization information as the signal gives an estimate of the systematic error.

- Normalization of the non-resonant background:
  As discussed in section VII B, we take the uncertainty of the amount and shape of the non-resonant background into account by assigning a $\pm 100\%$ error to its normalization.

- Polarization of non-resonant background:
  We measured the angular distributions of non-resonant events in the K^* sideband region 1.1 GeV to 1.45 GeV. To estimate the systematic error the fit was redone with isotropic angular distributions.

- Shape of uncorrelated $B \to J/\psi X$ and combinatorial background:
  The shape of the combinatorial background and the uncorrelated $B \to J/\psi X$ background is not uniform over the entire fit region (see Fig. 7). Its behavior at the phase space limit is also not well known. We therefore assign a systematic error of $\pm 50\%$ on the number of fitted events under the B mass peak.

- Polarization of uncorrelated $B \to J/\psi X$ and combinatorial background:
  The angular distributions of this background is measured in the B mass sidebands between 5.0 GeV and 5.25 GeV. A systematic error was determined in a similar way as in case of the non-resonant decays in redoing the fit with a uniformly-distributed background.

- Monte Carlo statistics:
  The uncertainty on the branching ratios due to the limited statistics of the Monte Carlo sample is about $\pm 2.8\%$ for $B^+ \to J/\psi K^+$ and $\pm 4.2\%$ for $B^0 \to J/\psi K^0$. For $B \to J/\psi K^*$ this error is negligible.

- Submode branching fractions:
  For both $\mathcal{B}(J/\psi \to e^+e^-)$ and $\mathcal{B}(J/\psi \to \mu^+\mu^-)$ we use the world average of $(6.01 \pm 0.19)\%$ [12]. The uncertainty in $\mathcal{B}(K^0_S \to \pi^+\pi^-)$ is negligible.

- Luminosity:
  There is an uncertainty of $\pm 1.8\%$ in each branching ratio measurement. from the uncertainty in luminosity.

	$10^3 \times \mathcal{B}(B \to J/\psi K^+)$	$10^3 \times \mathcal{B}(B \to J/\psi K^0)$	$10^3 \times \mathcal{B}(B \to J/\psi K^{*+})$	$10^3 \times \mathcal{B}(B \to J/\psi K^{*0})$
Tracking Efficiency	± 0.043	± 0.050	± 0.115	± 0.105
Lepton Identification Efficiency	± 0.058	± 0.050	± 0.076	± 0.071
Shape of Comb. Bkg.	± 0.007	± 0.002	± 0.020	± 0.008
Polarization of Comb. Bkg.			± 0.015	± 0.015
Normalization of $B \to J/\psi K^*$ Feed-Across			± 0.092	± 0.039
Polarization of $B \to J/\psi K^*$ Feed-Across			± 0.139	± 0.008
Normalization of $B \to J/\psi (K\pi)_{\mathrm{NR}}$			± 0.092	± 0.092
Polarization of $B \to J/\psi (K\pi)_{\mathrm{NR}}$			± 0.001	± 0.001
Efficiency Parameterization			± 0.013	± 0.013
Monte Carlo Statistics	± 0.022	± 0.027	± 0.007	± 0.008
$J/\psi \to l^+l^-$ Branching Ratio	± 0.034	± 0.029	± 0.045	± 0.042
Luminosity	± 0.020	± 0.017	± 0.025	± 0.025
Total	± 0.085	± 0.083	± 0.243	± 0.170

TABLE VII. Table of systematic uncertainties in the branching fraction measurements.

	$\Gamma_{\mathrm{L}}/\Gamma$	$\lvert A_\perp\rvert^2$	$\phi(A_\perp)$	$\phi(A_\parallel)$
Tracking Efficiency	< 0.001	± 0.001	± 0.001	< 0.001
Shape of Comb. Bkg.	< 0.001	< 0.001	< 0.001	< 0.001
Polarization of Comb. Bkg.	± 0.002	± 0.002	± 0.005	± 0.004
Normalization of $B \to J/\psi K^*$ Feed-Across	± 0.002	± 0.006	± 0.003	± 0.004
Polarization of $B \to J/\psi K^*$ Feed-Across	± 0.010	± 0.019	± 0.017	± 0.035
Normalization of $B \to J/\psi (K\pi)_{\mathrm{NR}}$	± 0.002	± 0.011	± 0.002	< 0.001
Polarization of $B \to J/\psi (K\pi)_{\mathrm{NR}}$	± 0.009	± 0.021	± 0.020	± 0.001
Efficiency Parameterization	± 0.032	± 0.028	± 0.022	± 0.007
Sum	± 0.035	± 0.042	± 0.030	± 0.036

TABLE VIII. Table of systematic uncertainties in the measurements of the decay amplitudes.

XI. CONCLUSION

We have performed different fits to the angular distributions in the $B \to J/\psi K^*$ modes. The fit of the full transversity angle distribution for all modes yields fractions of longitudinal polarization and parity-odd transverse polarization:

$$\Gamma_{\mathrm{L}}/\Gamma \;=\; |A_0|^2 = 0.52 \;\pm\; 0.07 \;\pm\; 0.04 \tag{12}$$
$$|P|^2 \;=\; |A_\perp|^2 = 0.16 \;\pm\; 0.08 \;\pm\; 0.04\,. \tag{13}$$

Setting $\phi(A_0) \equiv 0$, we find for the phases of the other decay amplitudes:

$$\phi(A_\perp) = -0.11 \;\pm\; 0.46 \;\pm\; 0.03 \tag{14}$$
$$\phi(A_\parallel) = 3.00 \;\pm\; 0.37 \;\pm\; 0.04\,. \tag{15}$$

Previous experiments have only measured $\Gamma_{\mathrm{L}}/\Gamma$ and obtained a variety of different results, as shown in Table IX. Note, that care has to be taken in averaging these measurements: The Cramér-Rao lower bound of the variance $\sigma^2(\Gamma_{\mathrm{L}}/\Gamma)$ of an unbiased estimate of $\Gamma_{\mathrm{L}}/\Gamma$ reaches 0 when $\Gamma_{\mathrm{L}}/\Gamma$ approaches 1, which explains the relatively small statistical errors of the ARGUS and previous CLEO II measurements as well as the apparently large difference between the previous and this CLEO measurement. In fact, two or three additional events at high $|\cos\theta_\psi|$ in the previous measurement would have given agreement between both CLEO results. The measurement presented here supersedes the previous CLEO II result, which is based on a subset of the data used for this analysis.

Experiment	$\Gamma_{\mathrm{L}}/\Gamma$
ARGUS [4]	$0.97 \pm 0.16 \pm 0.15$
CLEO II (1994) [1]	$0.80 \pm 0.08 \pm 0.05$
CDF [5]	$0.65 \pm 0.10 \pm 0.04$
This measurement	$0.52 \pm 0.07 \pm 0.04$

TABLE IX. Comparison of results for $\Gamma_{\mathrm{L}}/\Gamma$. This measurement includes the CLEO II (1994) data sample as a subset.

The results for the parity-odd component and the phases of the decay amplitudes are the first measurements of these quantities so far. The low value for the parity-odd component gives a good prognosis for using the $B^0 \to K^0_S\pi^0$ CP eigenstate decay for CP violation studies at asymmetric B factories and for obtaining a measurement of the unitarity angle β. The phases of the decay amplitudes are measured to be close to zero or π, giving no evidence for strong final state interactions.

For the branching fractions of the exclusive $B \to J/\psi K^{(*)}$ decays, we obtain the following results:

$$\mathcal{B}(B^+ \to J/\psi K^+) = (\,1.08\, \pm\, 0.09\, \pm\, 0.09\,) \times 10^{-3} \tag{16}$$

$$\mathcal{B}(B^0 \to J/\psi K^0) = (\,0.92\, {}^{+0.17}_{-0.15}\, \pm\, 0.08\,) \times 10^{-3} \tag{17}$$

$$\mathcal{B}(B^+ \to J/\psi K^{*+}) = (\,1.41\, \pm\, 0.20\, \pm\, 0.24\,) \times 10^{-3} \tag{18}$$

$$\mathcal{B}(B^0 \to J/\psi K^{*0}) = (\,1.32\, \pm\, 0.15\, \pm\, 0.17\,) \times 10^{-3}\,. \tag{19}$$

These values agree very well with recent measurements from CLEO [1] and CDF [6], with somewhat smaller errors.

When calculating the ratio of pseudoscalar to vector meson production we eliminate common systematic errors and find, assuming isospin invariance,

$$R \;=\; \frac{\mathcal{B}(B \to J/\psi K^*)}{\mathcal{B}(B \to J/\psi K)} \;=\; 1.36\, \pm\, 0.17\, \pm\, 0.11\,, \tag{20}$$

in good agreement with the CDF result of $R = 1.53 \pm 0.31 \pm 0.09$ [6]. These new measurements of R and $\Gamma_{\rm L}/\Gamma$, together with the measurement of the phases, are consistent with the factorization hypothesis for internal spectator decays.

XII. ACKNOWLEDGMENTS

We gratefully acknowledge the effort of the CESR staff in providing us with excellent luminosity and running conditions. J.P.A., J.R.P., and I.P.J.S. thank the NYI program of the NSF, M.S thanks the PFF program of the NSF, G.E. thanks the Heisenberg Foundation, K.K.G., M.S., H.N.N., T.S., and H.Y. thank the OJI program of DOE, J.R.P, K.H., and M.S. thank the A.P. Sloan Foundation, and A.W., and R.W. thank the Alexander von Humboldt Stiftung for support. This work was supported by the National Science Foundation, the U.S. Department of Energy, and the Natural Sciences and Engineering Research Council of Canada.

REFERENCES

[1] M.S. Alam *et al.* (CLEO Collaboration), Phys. Rev. D **50** (1994) 43.
[2] M. Gourdin, A.N. Kamal, and X.Y. Pham, Phys. Rev. Lett. **73** (1994) 3355.
[3] R. Aleksan, A. Le Yauoanc, L. Oliver, O. Pène, and J.C. Raynal, Phys. Rev. D **51** (1995) 6235.
[4] H. Albrecht *et al.* (ARGUS Collaboration), Phys. Lett. B **340** (1994) 217.
[5] F. Abe *et al.* (CDF Collaboration), Phys. Rev. Lett. **75** (1995) 3068.
[6] F. Abe *et al* (CDF Collaboration), FERMILAB-PUB-96-119-E (1996).
[7] B. Barish *et al.* (CLEO Collaboration), Phys. Rev. D **51** (1995) 1014, with $\tau_{B^+}/\tau_{B^0} = 1.02 \pm 0.05$ [12].
[8] A. Bohr, Nucl. Phys. **10** (1959) 486.
[9] A.S. Dighe, I. Dunietz, H.J. Lipkin and J.L. Rosner, Phys. Lett. B **369** (1996) 144.
[10] Y. Kubota, *et al.*, Nucl. Instrum. Meth. **A320**, 66–113 (1992).
[11] M. Bishai *et al.* (CLEO Collaboration), Phys. Lett. B **369** (1996) 186.
[12] R.M. Barnett *et al.* (Particle Data Group), Phys. Rev. D **54** (1996) 1.